Thermoelectric Properties of Porous SiC/SiO_2/C Composite from Carbonized *Cryptomeria japonica* Wood

Joko Sulistyo, Hiroyuki Kitagawa, and Sri Nugroho Marsoem

Abstract

Electric power generation by thermoelectric material utilizing radiated heat of from roof's house, engine and others is potential clean energy in tropical areas such as Indonesia. In this study, thermoelectric materials such as silicon carbide (SiC/SiO_2/C) composites were developed from carbonized *Cryptomeria japonica* wood infiltrated ethyl silicate-40 by sintering at 1400, 1600 and 1800 ºC for 30 min under N_2 atmosphere. This study aimed to examine the morphology, microstructure and thermoelectric properties of porous SiC/SiO_2/C composites. SiC/SiO_2/C composites sintered at 1600 ºC with low value of thermal conductivity was potential for the development of thermoelectric material. The oxidation of SiC/SiO_2/C composite sintered at 1600 °C which removed parts of residual silica and carbon, transformed the composite exhibiting p-type semiconductor with low values of Seebeck coefficient of to that exhibiting n-type semiconductor with high values Seebeck coefficient. A maximum of figure of merit of 6.25 x 10^{-5} K^{-1} was obtained at 140 ºC in the oxidized SiC/SiO_2/C composite sintered at 1600 °C. The comparatively high figure of merit indicates the potentiality the material for thermoelectric purpose.

Keywords: Thermoelectric properties, silicon carbide, carbonized wood, silica.

Introduction

Recently the development of green and clean energy from biomass has received a great attention for replacing fossil fuels. One of the biggest concerns associated with the development of green and clean energy is to reduce the amount of carbon in the atmosphere and minimize the impact on global climate change. Various alternative energy sources have been studied for example the generation of liquid fuels from biomass conversion such as bio-etanol (Sassner *et al.* 2008), bio-diesel (Oliveira *et al.* 2009), bio-oil by a fast pyrolysis (Balat *et al.* 2009), and aromatics by a catalytic fast pyrolysis (Carlson *et al.* 2009; French and Czernik 2010). Another potential energy is electric power generation using thermal or heat as initial energy form that is defined as thermoelectric power (Carpenter 2014). Indonesia as a tropical country with the long daylight provides potential the heat radiated from houses' roofs and walls. The other sources of heat are from engines of million motorcycles and cars or factories. The implementation of the electric power generation from the heat of houses will support the development of smart houses in which several electronic devices such as sensors, and others will be powered by this kind clean energy.

Thermoelectric power conversion employs thermoelements based on the effects of origination of thermoelectromotive forces (Anatychuk 2012). Thermal conduction for heat releasing from hot and cold side cause electrons move from cold to hot side in the p-type semiconductor, and from hot to cold side in the n-type semiconductor. It has been reported that porous SiC/C composite from carbonized wood which was prepared at 1400 °C for 30 min generated thermoelectric power with a maximum figure of merit of 3.38 x 10^{-7} K^{-1} at 200 ºC (Fujisawa *et al.* 2005). The open porous foam structure of thermoelectric oxide materials such as $Ca_3CO_4O_9$ makes the possibility to design efficient thermoelectric modules for waste heat sources (Noudem *et al.* 2008). The direct large area physical contact of thermoelectric foam elements with hot media will make them efficient electric power generators. The open porous thermoelectric materials with introduced porosities can be good candidates to confine phonons (lattice vibrations) in order to reduce the thermal conductivity if the pores can be made sufficiently small.

Porous SiC/SiO_2/C composites were produced from carbonized wood submerged in etylsilicate-40 solution under vacuum of 1 kPa following by a pre-treatment at room temperature that determined a solid-solid reaction during the sintering at 1400 – 1800 °C (Sulistyo *et al.* 2010). The purpose of this study was to examine the morphology, microstructure and thermoelectric properties of porous SiC/SiO_2/C composites. Furthermore, the effect of oxidation of SiC/SiO_2/C composite was studied on the improvement of the thermoelectric properties. The morphology was observed by scanning electron microscope (SEM). The microstructure was analyzed by Raman spectroscopy and X-ray diffraction. The thermal conductivities were measured by a laser flash method. The thermoelectrical properties were measured by thermoelectric measurement apparatus.

Materials and Methods

Preparation of SiC/SiO_2/C Composites

Sugi (*Cryptomeria japonica*) wood particles were heated at a rate of 4 ºC/min up to 700 ºC in a laboratory scale electric furnace. The particles were held at 700 ºC for 1 h under a N_2 gas flow of 100 mL/min. The resulting carbonized wood was then granulated using a blender and

sieved to yield particle sizes of 45~150 µm. A silica solution was prepared by diluting ethylsilicate-40 (Colcoat, Japan) with ethyl alcohol to obtain a 15% SiO_2 concentration by weight. The carbonized wood was submerged in the silica solution and held under a vacuum of 1 kPa for 90 min. The carbonized wood infiltrated with ethylsilicate-40 was then simply kept at room temperature until it dried. The final SiO_2 content calculated by the molar ratio was found to be 50% based on the dry charcoal weight. A dry weight of 1 g of carbonized wood infiltrated with SiO_2 was then placed into a 10 mm-internal-diameter graphite die with a length of 5 cm equipped with two graphite punches with a total length of 5 cm. To evaluate the effect of sintering temperature, SiC/SiO_2/C composites were heated to 1400, 1600, and 1800 ºC at a rate of 250 ºC/min with a holding time of 30 min under a pressure of 15 MPa and a N_2 gas flow of 1 L/min using a pulse current sintering device (VCSP II, SS Alloy, Hiroshima), hereafter denoted as non-oxidized SiC/SiO_2/C composite, respectively. The 5-mm-thickness samples obtained were cut into discs with a thickness of approximately 0.8 mm. Some samples prepared at 1600 ºC were oxidized at 900 ºC for 2 hr, in order to determine the improvement of thermoelectric properties, denoted as oxidized SiC/SiO_2/C composite. The bulk density of these samples with and without oxidation treatment was determined by the Archimedes method.

Characterization

The microstructure of non-oxidized and oxidized samples was analyzed using Raman spectroscopy (Renishaw inVia) with an air-cooled CCD detector. An argon laser with a wavelength of 514.5 nm was used as an excitation source. The spectra were measured in the 400~1,800 cm^{-1} range. Seven 10-s accumulations were collected to give an adequate signal to-noise ratio. The wave number was calibrated using the 520 cm^{-1} line of a silicon wafer. Spectral processing was performed using WiRE 2 software. X-ray diffraction (XRD, Rigaku-RINT-ultra X18) at 45 kV and 200 mA was used to determine the crystalline phase formed during sintering in non-oxidized and oxidized composite prepared at 1600 ºC. The data were collected as continuous scans, with a step size of 0.02º 2θ and a scan rate of 1º 2θ /min between 10 and 90º 2θ. The bulk samples were analyzed without powdering since a random orientation of crystallites was assumed to be already present.

The morphology of samples with and without oxidation treatment was observed using scanning electron microscopy (SEM, JEOL-JSM-5310). The samples were observed directly without any coating. The thermal diffusivity (α) and the specific heat (C_p) were measured under a vacuum at room temperature and in a temperature range from room temperature to 150 ºC by the laser flash method using a thermal constant analyzer (Ulvac, TC-7000H). The thermal conductivity (K_T) was calculated by the following equation:

$$K_T = \rho C_p \alpha \quad \text{..... (1)}$$

where ρ is the bulk density of the specimen (g/cm^3), C_p is specific heat ((J/g)/K), and α is the thermal diffusivity (m^2/s). The Seebeck coefficients and the electrical conductivity were measured under a vacuum in a temperature range from room temperature to 150 ºC using a Seebeck coefficient/electrical resistance measuring system. The figure of merit of the specimen was calculated using the following equation:

$$Z = \frac{S^2 \sigma}{K_T} \quad \text{.....(2)}$$

where Z is figure of merit (K−1), S is Seebeck coefficient (V/K), σ is electrical conductivity (Ω^{-1} m^{-1}), K_T is thermal conductivity (W/(m K)).

Results and Discussion

The Raman spectra are shown in Fig. 1. In non-oxidized SiC/SiO_2/C samples prepared at 1600 and 1800 ºC and oxidized sample prepared at 1600 ºC, the transverse optic (TO) peak was observed at around 783~796 cm^{-1}, corresponding to phonon mode of cubic β-SiC (Shiryaev *et al.* 2008) (Fig. 1a and b). The TO peak became more intense and narrower as the heat treatment temperature increased to 1800 ºC. Narrowing of the TO peak in both SiC/SiO_2/C samples heated at 1600 and 1800 ºC is related to ordering of the β-SiC crystals. The Raman spectra of non-oxidized samples heated at 1400 ºC did not appear the TO peak, indicating less formation of β-SiC. The Raman spectra of non-oxidized composite samples exhibited broad D and G bands at around 1349~1357 and 1582~1589 cm^{-1}, respectively, attributed to carbon material with a turbostratic structure (Ishimaru *et al.* 2007). The width of D and G band peaks corresponds to the degree of order in the carbon microstructure. The narrowing D and G bands was found with the increase of sintering temperature indicating the improvement the amount of ordering in the carbon microstructure. The D and G bands were not observed in the spectra of composite sample that had been oxidized, indicating that parts of the residual carbon had been removed.

The XRD patterns of non-oxidized and oxidized SiC/SiO_2/C composites prepared at 1600 ºC as shown in Fig. 2. Major diffraction peaks are observed at around 2θ = 14 and 17º, corresponding to the SiO_2 crystal phase, around 2θ = 26, 44, and 79º, corresponding to the (002), (101), and (110) turbostratic carbon phase, respectively, and around 2θ = 35, 42, 60, and 72º, corresponding to the (111), (200), (220), and (311) reflections of the cubic β-SiC phase (Cheung and Ng 2007); Shin and Exarhos 2007). As can be seen from the XRD patterns, both non-oxidized and oxidized composite samples prepared at 1600 ºC contained 3 crystal

phases including SiO_2, turbostratic carbon and β–SiC, supporting the Raman spectroscopy analysis. The intensity of peaks of SiO_2 crystal phase and turbostratic carbon decreased with the oxidation of sample at 900 ºC for 2 h due to residual silica (SiO_2) and carbon decreased. After the oxidation treatment the residual silica and carbon was still exist in the composite.

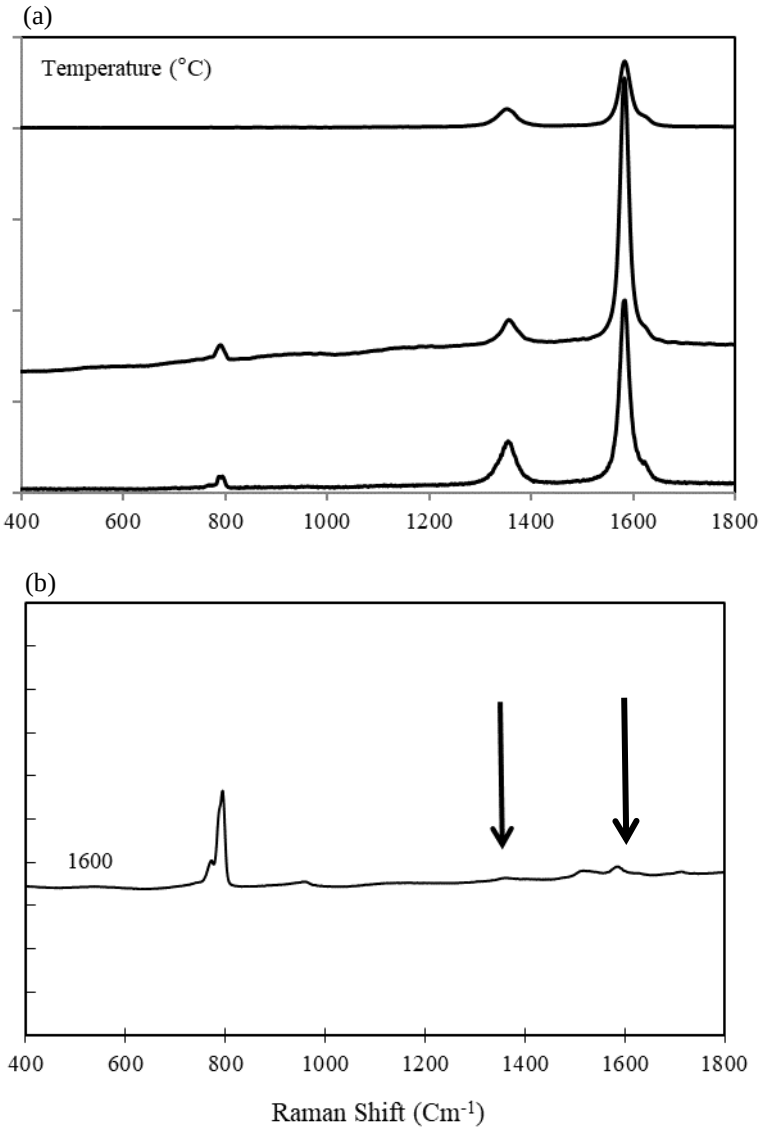

Figure 1. Raman spectra in the ranges of 400~1800 cm^{-1} of (a) non-oxidized $SiC/SiO_2/C$ composite samples prepared at different sintering temperatures and (b) oxidized $SiC/SiO_2/C$ composite sample prepared at 1600 ºC. *TO* transverse optic, *D band* disorder, *G band* graphite. The arrows indicate the less intensive of the transverse optic peak.

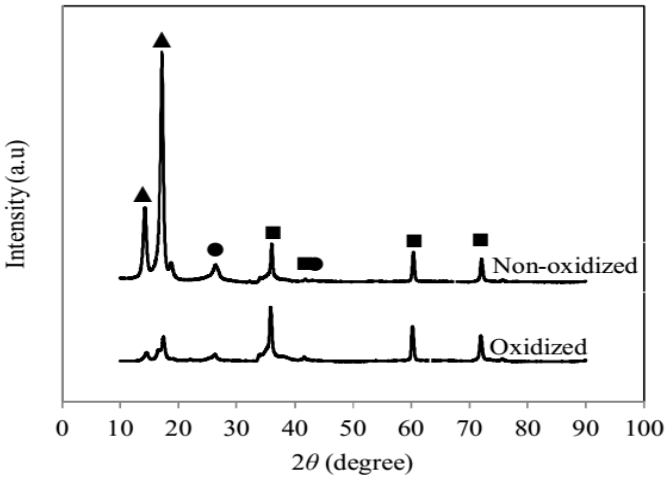

Figure 2. X-ray diffraction pattern of non-oxidized and oxidized SiC/SiO_2/C composite prepared at 1600 ºC. (●) C, (■) β-SiC, (▲) SiO_2.

Figure 3 (a-c) shows SEM images of the morphology of non-oxidized SiC/SiO_2/C composites prepared at 1400, 1600 and 1800 ºC. In the non-oxidized SiC/SiO_2/C composite prepared at 1400 and 1600 ºC the particles were closely packed with spherical bodies distributed over the surface of the particles, as indicated by arrows, while in the samples that had been sintered at 1800 ºC the particles were even more closely packed with smaller spherical bodies found on the surface of particles, as shown by arrow in Fig. 3 (c). It is considered that the morphological difference depends on the sintering temperature. Figure 3 (d) shows SEM images of the morphology of the SiC/SiO_2/C composites sintered at 1600 ºC followed by an oxidation at 900 ºC for 2 h. The pores were clearly visible on the surface of the particles, as indicated by arrow. Oxidation of the residual silica and carbon of sample influenced the pore development. The morphology of oxidized composite possessed more porosity due to the removal of the excess silica and carbon comparing to that of non-oxidized composites. The removal of parts of the excess silica and carbon was confirmed by the disappearing of D and G bands on the Raman spectra and the decreasing intensity of both crystal phases on the XRD patterns.

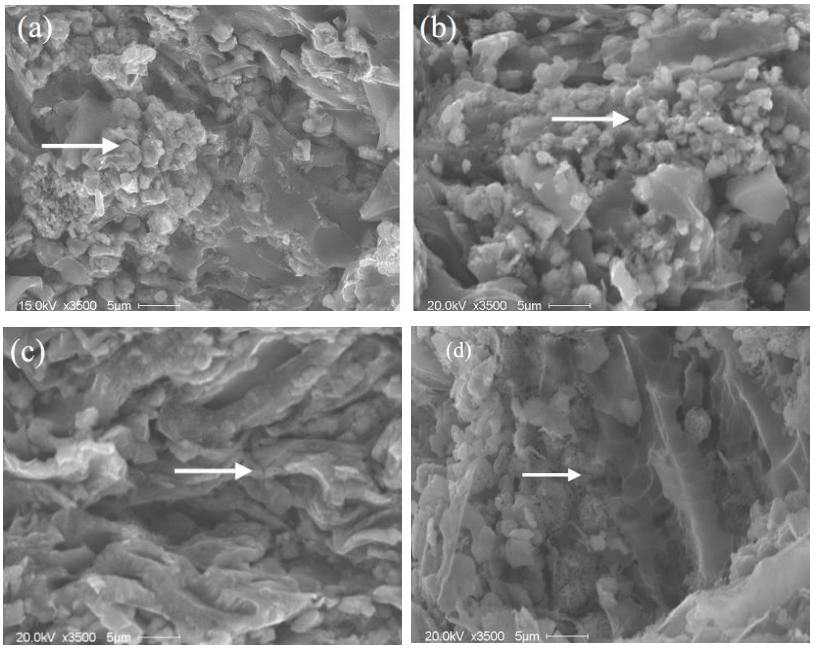

Figure 3. SEM images of non-oxidized SiC/SiO_2/C composites sintered at (a) 1400, (b) 1600, (c) 1800 ºC and oxidized SiC/SiO_2/C composite sintered at (d) 1600 ºC.

The bulk density of sample prepared at 1800 ºC showed drastically increase value compared with the others samples as shown in Fig.4. The high density of samples prepared at 1800 ºC were consistent with SEM observation which is showed the close packed particles with small spherical bodies on this sample. The bulk density of sample heated at 1600 ºC was lower than that prepared at 1400 ºC. The large spherical bodies on the surface of particles and large pore size that was consistent with the SEM image influenced the low bulk density of sample prepared at 1600 ºC. The oxidation of the excess silica and carbon that opened the large pore size, as shown in SEM image, decreased substantially the bulk density of sample prepared at 1600 ºC.

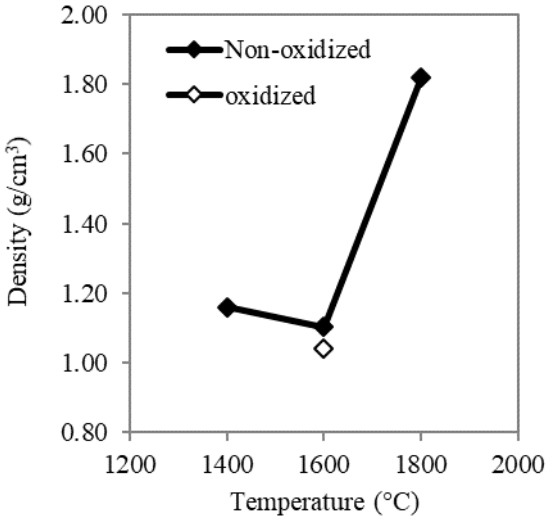

Figure 4. Relationship between bulk density of non-oxidized and oxidized $SiC/SiO_2/C$ composites and sintering temperature.

Figure 5 shows the temperature dependence of the thermal conductivity of non-oxidized $SiC/SiO_2/C$ samples prepared at 1400, 1600 and 1800 ºC and also oxidized $SiC/SiO_2/C$ sample prepared at 1600 ºC. The thermal conductivity of the oxidized sample prepared at 1800 ºC was higher than those prepared at 1400 and 1600 ºC, as a result of a greater amount of β-SiC crystals indicated by the appearing the TO peak on the Raman spectra and the intensity of peaks 2θ = 35, 42, 60, and 72º on the XRD patterns. The thermal conductivity of the non-oxidized $SiC/SiO_2/C$ sample prepared at 1800 ºC decreased with the increase of measuring temperature. The porosity contribution is dominated in the decreasing of thermal conductivity with the increasing temperature (Pappacena *et al.* 2007). The thermal conductivity of oxidized $SiC/SiO_2/C$ sample prepared at 1600 ºC was much lower than that non-oxidized sample. The thermal conductivity decreases with increasing porosity (Pappacena *et al.* 2007; Wang *et al.* 2007; Wei *et al.* 2007) as discussed previously. Pores influence the thermal conductivity of material as heat conduction is being scattered by pores. $SiC/SiO_2/C$ composite prepared at 1600 ºC with and without oxidation that exhibited low values of thermal conductivity was potential candidate for thermoelectric material. These sample were then measured its Seebeck coefficient as follow.

Figure 6 shows the temperature dependence of the Seebeck coefficient of non-oxidized and oxidized $SiC/SiO_2/C$ composite samples prepared at 1600 ºC. The $SiC/SiO_2/C$ composite prepared at 1600 ºC, without oxidation (non-oxidized sample), showed a positive sign which was expected to be p-type semiconductor. The maximum value of Seebeck coefficient of $SiC/SiO_2/C$ composite without oxidation was 7.51 μVK^{-1} at measuring temperature of 150 °C which was lower than that of polycrystalline 3C-SiC films with value about 51 μVK^{-1} at measuring temperature of 244 °C (Ivanova *et al.* 2006), SiC foam with value about 120 μVK^{-1} at measuring temperature of 800 °C (Wei *et al.* 2007), indium arsenide nanofilm with value around 55 μVK^{-1} at similar measuring temperature (Mavrokefalos *et al.* 2007) and β-$FeSi_2$ with SiO_2 and TiO dispersion with value of 200 μVK^{-1} at measuring temperature of 400 °C (Ito *et al.* 2006). The oxidation of $SiC/SiO_2/C$ composite (oxidized sample) showed a negative sign corresponding to an n-type semiconductor. The oxidation treatment transformed p-type to n-type semiconductor and also improved much higher the Seebeck coefficient of $SiC/SiO_2/C$ composite than that of $SiC/SiO_2/C$ composite without oxidation. It has been reported that porous SiC ceramics have a high Seebeck coefficient (Fujisawa *et al.* 2008). The oxidation treatment removed parts of residual silica and carbon in $SiC/SiO_2/C$ composite, as confirm by Raman spectra and XRD pattern, and changed the microstructure by developing large amount of pores in the composite, as confirm by SEM image. The highest Seebeck coefficient value of $SiC/SiO_2/C$ composite

at measuring temperature of 150 °C was comparable with porous SiC composite (Fujisawa *et al.* 2008) and with CSMO foam with value of -178 μVK^{-1} (Noudem *et al.* 2008).

The electrical conductivity and figure of merit of oxidized SiC/SiO_2/C composite sample prepared at 1600 ºC in relationship with measurement temperature as shown in Fig. 7 (a-b). The electrical conductivity increased with the increase in measurement temperature which is similar with previous report in SiC/C composite (Fujisawa *et al.* 2005). The figure of merit of oxidized SiC/SiO_2/C composite which was calculated using Eq. (2) also increased as the measurement temperature increased. A maximum value of the figure of merit of 6.25 x 10^{--5} K^{-1} was obtained at 140 ºC in the oxidized SiC/SiO_2/C composite sample prepared at 1600 ºC. The result of maximum figure of merit of oxidized SiC/SiO_2/C composite at measurement temperature range from 30~150 ºC was higher than that on the previous result of SiC/C composite that obtained 3.38 x 10^{-7} K^{-1} at 200 ºC (Fujisawa *et al*. 2005), SiC foam that obtained 1 x 10^{-7} K^{-1} at 800 ºC (Wei *et al.* 2007), and porous SiC composite that obtained 2.01 x 10^{-5} K^{-1} at 700 ºC (Fujisawa et al. 2008).

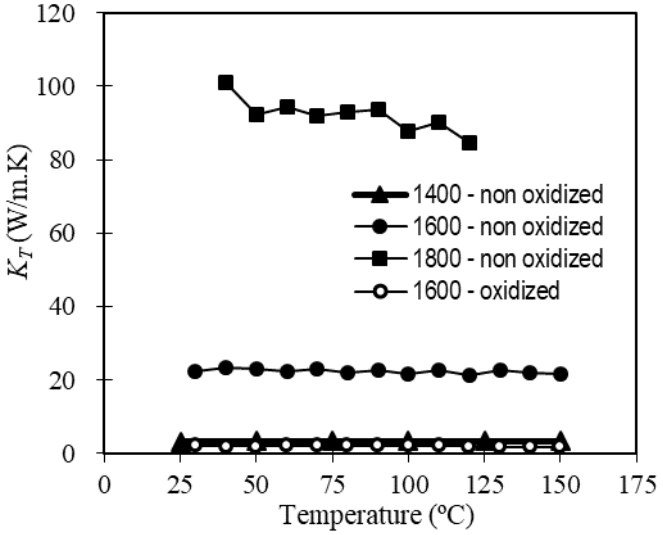

Figure 5. Thermal conductivities of non-oxidized SiC/SiO_2/C composite samples prepared at 1400, 1600 and 1800 ºC and oxidized SiC/SiO_2/C composite sample prepared at 1600 ºC measured in the ranges of 30~150 ºC

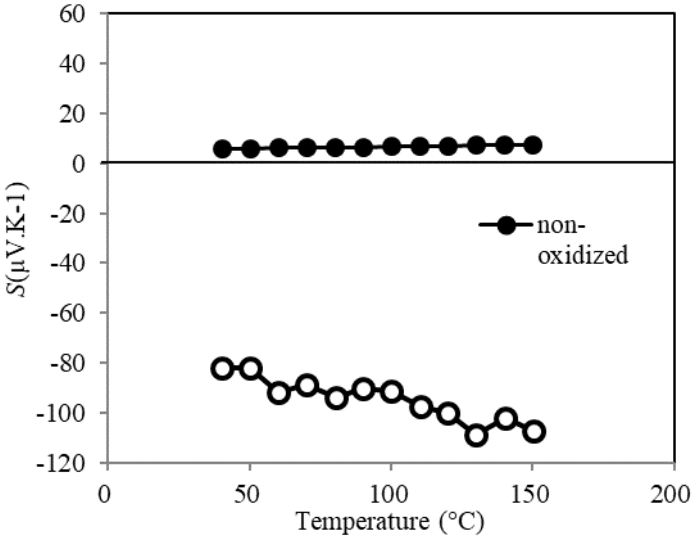

Figure 6. Seebeck coeficient of oxidized SiC/SiO_2/C composite sample prepared at 1600 ºC measured in the ranges of 30~150 ºC.

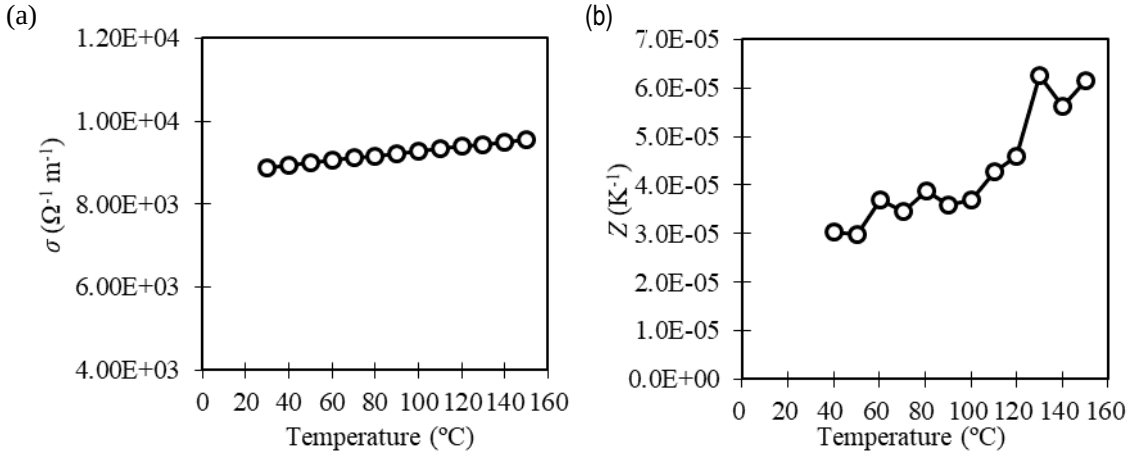

Figure 7. (a) Electrical conductivity and (b) figure of merit of oxidized SiC/SiO_2/C composite sample prepared at 1600 ºC measured in the ranges of 30~150 ºC.

Conclusions

Porous SiC/SiO_2/C composites were developed from carbonized wood infiltrated with ethylsilicate-40 using a pulse current sintering apparatus at temperature range from 1400~1800 °C. The SiC/SiO_2/C composite sintered at 1600 °C with the low value of thermal conductivity was potential for thermoelectric material. The oxidation of SiC/SiO_2/C composite sintered at 1600 °C which removed parts of residual silica and carbon, transformed the composite exhibiting p-type semiconductor with low values of Seebeck coefficient to that exhibiting n-type semiconductor with high value Seebeck coefficient. A maximum of figure of merit of 6.25 x 10^{-5} K^{-1} was obtained at 140 ºC in the oxidized SiC/SiO_2/C composite sintered at 1600 °C. This achieved figure of merit suggests that this treatment would suitable for further development in term of thermoelectric materials.

References

Anatychuk, L.I. 2012. Thermoelectris and Its Energy Harvesting: Materials, Preparation, and Characterization. In Thermoelectrics. D.M. Rowe (ed.). CRC Press. Boca Raton.

Balat, M.; M. Balat; E. Kirtay; H. Balat. 2009. Main routes for the thermo-conversion of biomass into fuels and chemicals. Part 1: Pyrolysis systems. Energy Conversion and Management 50(12): 3147-3157.

Carlson, T.R.; G.A. Tompsett; W.C. Conner; G.W. Huber. 2009. Aromatic production from catalytic fast pyrolysis of biomass-derived feedstocks. Topics in Catalysis 52: 241–252.

Carpenter, N.E. , 2014. Chemistry of Sustainable Energy. CRC Press, Boca Raton. pp.1-18.

Cheung, T.L.Y.; D.H.L. Ng. 2007. Conversion of bamboo to biomorphic composites containing silica and silicon carbide nanowires. Journal of American Ceramic Society 90: 559-564.

French, F.; S. Czernik. 2010. Catalytic pyrolysis of biomass for biofuels production. Fuel Processing Technology 91: 25-32.

Fujisawa, M.; T. Hata; P. Bronsveld; V. Castro; F. Tanaka; H. Kikuchi; Y. Imamura. 2005. Thermoelectric properties of SiC/C composites from wood charcoal by pulse current sintering. Journal of the European Ceramic Society 25: 2735-2738.

Fujisawa; M.; T. Hata; H. Kitagawa; P. Bronsveld; Y. Suzuki; K. Hasezaki; Y. Noda; Y. Imamura. 2008. Thermoelectric properties of porous SiC/C composites. Renewable Energy 33: 309-313.

Ishimaru, K.; T. Hata; P. Bronsveld; Y. Imamura. 2007. Microsectioning study of carbonized wood after cell wall sectioning Journal of Materials Science 42: 2662-2668.

Ivanova, L.M.; P.A. Aleksandrov; K.D. Demakov. 2006. Thermoelectric properties of vapor-grown polycrystalline cubic SiC. Inorganic Materials 42: 1205-1209.

Ito, M.; T. Tanaka; S. Hara. 2004. Thermoelectric properties of β-$FeSi_2$ with electrically insulating SiO_2 and conductive TiO dispersion by mechanical alloying. Journal of Applied Physics 95: 6209-6215.

Mavrokefalos, A.; M.T. Pettes; F. Zhou; L. Shi. 2007. Four-probe measurements of the in-plane thermoelectric properties of nanofilms. The Review of Scientific Instruments 78(3): 034901 - 034901-6.

Noudem, J.G.; S. Lemonnier; M. Prevel; E.S. Reddy; E. Guilmeau; C. Goupil. 2008. Thermoelectric ceramics for generators. Journal of the European Ceramic Society 28: 41-48.

Oliveira, J.S. de; P.M. Leite; L.B. de Souza; V.M. Mello; E.C. Silva; J.C. Rubim; S.M.P. Meneghetti; P.A.Z Suarez. 2009. Characteristics and composition of *Jatropha gossypiifolia* and *Jatropha curcas* L. oils and application for biodiesel production. Biomass and Bioenergy 33 (3): 449-453.

Pappacena, K.E.; K.T. Faber; H. Wang; W.D. Porter. 2007. Thermal conductivity of porous silicon carbide derived

from wood precursors. Journal of the American Ceramic Society 90 (9): 2855-2862

Sassner, P.; G. Zacchi. 2008. Integration options for high energy efficiency and improved economics in a wood-to-ethanol process. Biotechnology for Biofuels 4: 1-11.

Shin, Y.; G.J. Exarhos. 2007. Conversion of cellulose materials into nanostructured ceramics by biomineralization. Cellulose 14: 269-279..

Sulistyo, J.; T. Hata; H. Kitagawa; P. Bronsveld; M. Fujisawa; K. Hashimoto; Y. Imamura. 2010. Electrical and thermal conductivity of porous $SiC/SiO_2/C$ with different morphology from carbonized wood. Journal of Materials Science 45: 1107-1116.

Shiryaev, A.A.; M. Wiedenbeck; V. Reutsky; V.B. Polyakov; N.N. Melnik; A.A. Lebedev; R. Yakimova. 2008. Isotopic heterogeneity in synthetic and natural silicon carbide. Journal of Physics Chemistry Solid 69: 2492-2498.

Wang, S.Y.; C.P. Hung. 2003. Electromagnetic shielding efficiency of the electric field of charcoal from six wood Species. Journal of Wood Science 49: 450-454.

Wei, W.; J. Li; H. Zhang; X. Cao; C. Tian; J. Zhang. 2007. Macrostructural influence on the thermoelectric properties of SiC ceramics. Scripta Materialia 57(12): 1081-1084.

Joko Sulistyo and Sri Nugroho Marsoem
Dept. of Forest Products Technology, Faculty of Forestry,
Universitas Gadjah Mada,
Jl. Agro No. 1, Bulaksumur, Yogyakarta, Indonesia
Tel. : +62-274-6491428
Fax. : +62-274-550541
Email : jsulistyo@ugm.ac.id

Hiroyuki Kitagawa
Department of Materials Science, Shimane University,
Nishikawatsu 1060, Matsue, Shimane 690-8504, Japan